OPEN ACCESS Freely available online

PLOS ONE

Exploring Three PIPs and Three TIPs of Grapevine for Transport of Water and Atypical Substrates through Heterologous Expression in *aqy-null* Yeast

Farzana Sabir[1,2], Maria José Leandro[1], Ana Paula Martins[1,2], Maria C. Loureiro-Dias[1], Teresa F. Moura[2], Graça Soveral[2,3], Catarina Prista[1]*

1 Centre for Botany Applied to Agriculture (CBAA), Instituto Superior de Agronomia, University of Lisbon, Lisbon, Portugal, **2** Instituto de Investigação do Medicamento (iMed.ULisboa), Faculdade de Farmácia, Universidade de Lisboa, Lisboa, Portugal, **3** Dept. de Bioquímica e Biologia Humana, Faculdade de Farmácia, Universidade de Lisboa, Lisboa, Portugal

Abstract

Aquaporins are membrane channels that facilitate the transport of water and other small molecules across the cellular membranes. We examined the role of six aquaporins of *Vitis vinifera* (cv. Touriga nacional) in the transport of water and atypical substrates (other than water) in an *aqy-null* strain of *Saccharomyces cerevisiae*. Their functional characterization for water transport was performed by stopped-flow fluorescence spectroscopy. The evaluation of permeability coefficients (P_f) and activation energies (*Ea*) revealed that three aquaporins (*Vv*TnPIP2;1, *Vv*TnTIP1;1 and *Vv*TnTIP2;2) are functional for water transport, while the other three (*Vv*TnPIP1;4, *Vv*TnPIP2;3 and *Vv*TnTIP4;1) are non-functional. TIPs (*Vv*TnTIP1;1 and *Vv*TnTIP2;2) exhibited higher water permeability than *Vv*TnPIP2;1. All functional aquaporins were found to be sensitive to $HgCl_2$, since their water conductivity was reduced (24–38%) by the addition of 0.5 mM $HgCl_2$. Expression of *Vitis* aquaporins caused different sensitive phenotypes to yeast strains when grown under hyperosmotic stress generated by KCl or sorbitol. Our results also indicate that *Vitis* aquaporins are putative transporters of other small molecules of physiological importance. Their sequence analyses revealed the presence of signature sequences for transport of ammonia, boron, CO_2, H_2O_2 and urea. The phenotypic growth variations of yeast cells showed that heterologous expression of *Vitis* aquaporins increased susceptibility to externally applied boron and H_2O_2, suggesting the contribution of *Vitis* aquaporins in the transport of these species.

Citation: Sabir F, Leandro MJ, Martins AP, Loureiro-Dias MC, Moura TF, et al. (2014) Exploring Three PIPs and Three TIPs of Grapevine for Transport of Water and Atypical Substrates through Heterologous Expression in *aqy-null* Yeast. PLoS ONE 9(8): e102087. doi:10.1371/journal.pone.0102087

Editor: Dan Zilberstein, Technion-Israel Institute of Technology Haifa 32000 Israel, Israel

Received April 17, 2014; **Accepted** June 15, 2014; **Published** August 11, 2014

Data Availability: The authors confirm that all data underlying the findings are fully available without restriction. All gene sequences are available from GeneBank VvTnPIP1;4 accession = KJ697714, VvTnPIP2;1 accession = KJ697715, VvTnPIP2;3 accession = KJ697716, VvTnTIP1;1 accession = KJ697717, VvTnTIP2;2 accession = KJ697718, VvTnTIP4;1 accession = KJ697719.

Funding: This work is supported by Fundação para a Ciência e Tecnologia (FCT), Portugal (Post-Doctral grants-SFRH/BPD/89427/2012 to F. S. and SFRH/BPD/41812/2007 to M. J. L., Ciência 2007 to C. P. and project grant PTDC/AGR/AAM/099154/2008). The funders had no role in study design, data collection and analysis, decision to publish, or preparation of the manuscript.

Competing Interests: The authors have declared that no competing interests exist.

* Email: cprista@isa.ulisboa.pt

Introduction

Aquaporins play a crucial role in maintaining water and ion homeostasis of plants, essential for plant cell integrity, growth and survival in their ever-changing environment. These water channels can provide rapid and reversible changes to cells hydraulic conductance by modulating membrane water permeability [1]. Aquaporins belong to Major Intrinsic Proteins (MIPs) family and based on their sequence similarity and sub-cellular localization, plant aquaporins are divided in seven subfamilies: the plasma membrane intrinsic proteins (PIPs), the tonoplast intrinsic proteins (TIPs), the nodulin-26-like intrinsic proteins (NIPs), the small intrinsic proteins (SIPs), the GlpF-like intrinsic proteins (GIPs), the hybrid intrinsic proteins (HIPs) and the uncategorized X intrinsic proteins (XIPs) [2]. Studies on plant aquaporins revealed their role far beyond the membrane water transport. Besides water, they are reported to transport also other small molecules and/or gases of physiological importance (reviewed by [3]), suggesting their versatile functions in plants. Putative substrate specificities of aquaporins are generally assigned by the presence of specific amino acid residues at well-defined positions in the sequences [4].

Since aquaporins establish a tight association between water transport and plant development and adaptation under stress conditions, a rigorous regulation of aquaporin activity is essential to fine-tune the overall hydraulic conductivity in plants [5]. Expression of aquaporin genes can be altered under various environmental conditions as well as according to cell/tissue type and plant developmental stages [6]. Besides these initial regulatory steps of gene expression, the activity of translated and targeted aquaporin proteins can be further regulated by various post-translational modifications such as methylation, glycosylation, phosphorylation, membrane trafficking, heteromerization, and their gating can also be regulated by pH, divalent ions and membrane tension [7]. Various stress conditions like anoxia, salt and water stress have also been reported to affect the activity of aquaporins in plants (reviewed by [3,6]).

Vitis vinifera cv. Touriga nacional is an important Portuguese cultivar. This variety is a key ingredient in both dry red and fortified wines (particularly, Port wine). Grapevines are known to be extremely stress-tolerant plants, especially for dry environment [8]. In fact, deficit irrigation techniques are commonly used to achieve high fruit quality [9]. Since the water status of the plant greatly influences the fruit quality and hence the characteristics of wine [10], it is significant to study the molecular cell entry point of water, i.e. aquaporins in these plants. Release of full genomic sequence of grapevine revealed the occurrence of 28 genes encoding putative aquaporins in *V. vinifera* [11]. Comprehensive phylogenetic analyses of the deduced amino acid sequences suggest that the *V. vinifera* (cv. Cabernet Sauvignon and cv. Pinot Noir) aquaporins can be distributed in the four main subfamilies: PIPs (8 genes), TIPs (10 genes), NIPs (8 genes) and SIPs (2 genes) [12]. Despite being a very important economical plant, only few reports are available on *Vitis* aquaporins, explaining their quantitative expression in various rootstocks [13], during water stress [14,15] and their cloning and expression *in planta* [8,16] or in heterologous systems, such as *Xenopus* oocytes [1,12] and *S. cerevisiae* [17,18]. Although from a molecular point of view the presence of aquaporins can be easily recognized in a genome, their physiological role *in planta* is still difficult to understand. At transcript level, plant aquaporins respond variedly to stress, depending on the plant tissue/organ, cultivars/species and types/degree of stress [1], impairing the interpretation of the role of an individual aquaporin. To study the physiological role of each aquaporin, we used *S. cerevisiae* as a simple and well-characterized heterologous expression system [19]. The evaluation of water transport activity in intact yeast cells through stopped-flow fluorescence spectroscopy is already well-established [17,20].

The present work is focused on the cloning and expression of putative aquaporins (three PIPs and three TIPs) of *Vitis vinifera* (cv. Touriga nacional) in an *aqy-null* strain of *S. cerevisiae*. Their functional characterization for water transport was performed through stopped-flow spectroscopy. Further, tolerance/sensitivity of these aquaporins expressing strains was tested under hyperosmotic stress exerted by KCl or sorbitol. This study also includes the analysis of signature sequences for transport of atypical substrates and growth assays of yeast strains expressing *Vitis* aquaporins in the presence of these substrates, to explore their putative route of transport.

Materials and Methods

Yeast strain, plasmid and growth conditions

Saccharomyces cerevisiae 10560-6B *MATα leu2::hisG trp1::hisG his3::hisG ura3-52 aqy1::KanMX4 aqy2::HIS3* (from now on designated as *aqy-null*) was used as host strain for heterologous expression of putative aquaporins from *V. vinifera* cv. Touriga nacional. The centromeric plasmid pUG35 was used for cloning, conferring C-terminal GFP tagging, MET25 promoter and CYC1-T terminator [21]. For propagation of these plasmids, *Escherichia coli* DH5α strain was used as host [22]. *E. coli* transformants were grown in Luria-Bertani (LB) medium supplemented with ampicillin (100 μg ml^{-1}), at 37°C. The host *S. cerevisiae* strain (*aqy-null*) was maintained in YPD medium (5 g l^{-1} yeast extract, 10 g l^{-1} peptone, 20 g l^{-1} glucose and 20 g l^{-1} agar). Transformed yeast strains were grown and maintained in YNB medium without amino acids (DIFCO) with 2% (w/v) glucose supplemented with the adequate requirements for prototrophic growth [23].

Cloning and heterologous expression of *Vitis vinifera* aquaporins in *S. cerevisiae*

To clone the putative aquaporins from *V. vinifera* cv. Touriga nacional, their cDNA (kindly provided by Dr. Luísa Carvalho, ISA-ULisboa) amplification, cloning and expression in *S. cerevisiae* were performed according to previously described methods [17]. Primers used in this study are listed in Table S1.

Sequence analysis

Nucleotide sequences identified in the present study are submitted to National Center for Biotechnological Information (NCBI) (http://www.ncbi.nlm.nih.gov). These sequences were translated by ExPASy translate tool (http://web.expasy.org/translate/). Deduced amino acid sequences were analysed and compared with database sequences of *V. Vinifera* cv. Pinot noir, available at Grape Genome Browser (http://www.genoscope.cns.fr/externe/Genome Browser/Vitis/) and NCBI. Multiple protein sequence alignments were generated by using the ClustalX [24] and BioEdit [25] programs. Phylogenetic tree was constructed from the alignment of deduced amino acid sequences obtained from the present study and our previous study [17] with twenty-eight amino acid sequences of aquaporins of *V. vinifera* cv. Pinot noir, by MEGA5.1 software using neighbor-joining method [26]. Topology and hydrophobicity of deduced amino acid sequences were predicted by using various ExPASy tools e.g. TMHMM [27], HMMTOP [28] and TMPred [29].

All gene sequences are available from at GeneBank VvTnPIP1;4 accession = KJ697714, VvTnPIP2;1 accession = KJ697715, VvTnPIP2;3 accession = KJ697716, VvTnTIP1;1 accession = KJ697717, VvTnTIP2;2 accession = KJ697718, VvTnTIP4;1 accession = KJ697719.

To search the signature sequences for transport of atypical substrates, obtained amino acid sequences were grouped with reference sequences as per their reported substrates for transport, described by [4] and were aligned using ClustalX. Conserved amino acid residues at NPA, ar/R constriction and P1–P5 regions were determined from the alignment and matched with reference sequences of transporters of various substrates. Based on the conserved residues at these positions, selectivity profiles of cloned aquaporins were predicted.

Water transport assays of *Vitis* aquaporins expressed in *S. cerevisiae*

Functional analyses of heterologously expressed *Vitis* aquaporins for water conductivity were performed by stopped-flow fluorescence spectroscopy as previously described [17]. Briefly, yeast strains grown in liquid YNB medium were harvested at mid exponential phase ($OD_{640\ nm} \approx 1.0$) (Ultrospec 2100 pro, Amersham Biosciences) and incubated for 1 hour at 28°C in YPD medium (6 g l^{-1} wet weight). Further, cells were washed and re-suspended in ice-cold 1.4 M sorbitol (3 ml g^{-1} wet weight) and incubated on ice for at least 90 minutes. Cells were pre-loaded with the membrane permeable nonfluorescent precursor 5-(and-6)-carboxyfluorescein diacetate (CFDA), which is intracellularly hydrolyzed releasing the membrane impermeable fluorescent form. For water transport assays, hyperosmotic shocks were applied on stopped-flow apparatus (HI-TECH Scientific PQ/SF-53). Cells equilibrated with 1.4 M sorbitol were mixed with an equal volume of 2.1 M sorbitol. The resulting cell shrinkage caused a quenching of the fluorescence intensity. Signals were fitted to a single exponential, from which the rate constant (k) was calculated. Permeability coefficient (P_f) and activation energy (Ea) were estimated as described by [17,20].

Inhibition of water transport in *Vitis* aquaporins expressing yeast strains was tested with mercury chloride ($HgCl_2$), a well-known inhibitor of aquaporins. Yeast strains expressing functional *Vitis* aquaporins were incubated with $HgCl_2$ (0.5 and 1 mM, in 50 mM potassium citrate buffer, pH 5.0) for 15 and 30 minutes before the osmotic shock at 23°C. The yeast strain with the empty plasmid was treated in the same way and considered as control. Osmotic shocks were applied without and after incubation with $HgCl_2$ and the signals obtained were compared and used to calculate the P_f in both conditions.

Growth assays under osmotic stress and sensitivity tests on atypical substrates

S. cerevisiae strains harboring *Vitis* aquaporins were tested for their ability to grow under osmotic stress. Moreover, possibility to transport atypical substrates, such as ammonia, boron, hydrogen peroxide (H_2O_2) and urea was also investigated. Growth assays were performed on solid YNB medium (pH 5.0) supplemented with 2% (w/v) glucose. NaCl (0.5, 1.0 and 1.5 M), KCl (0.5, 1.0 and 1.5 M) and osmoequivalent concentration of sorbitol (0.84, 1.4 and 2.1 M) were added to growth media for osmotic stress experiments. Hydrogen peroxide (0.5, 0.75, 1.0, 1.5 and 2.0 mM) and boron (as boric acid, 20, 40, 50 and 60 mM), were used as atypical substrates for transport. Media with H_2O_2 was freshly prepared at the time of inoculation. Moreover, in order to test the putative transport of ammonia (1.0, 2.0 and 3.0 mM) and urea (1.0, 2.0, 2.5 and 3.5 mM), either of them was used as sole nitrogen source. Yeast strains were initially grown in liquid YNB medium supplemented with 2% (w/v) glucose, with orbital shaking (180 rpm) at 28°C, up to $OD_{640\ nm} \approx 1.0$ corresponding to 1×10^7 cells/ml. Cells were centrifuged and washed in sterile distilled water and re-suspended to $OD_{640\ nm} \approx 10$. Multi-well plates were prepared with serial 10-fold dilutions of the original concentrated culture, 3 µl suspensions was spotted with replica platter for 96-well plates device on plates containing YNB solid medium with ammonia, boric acid, H_2O_2 and urea, separately and incubated at 28°C. Strain with the empty plasmid (pUG35) was considered as control. Differences in growth phenotypes of yeast strains were recorded after 1 and 2 weeks of incubation.

Microscopy

For the localization of GFP-tagged proteins in *S. cerevisiae*, mid-exponential phase cells were observed under Leitz Wetzlar Germany 513558 epifluorescence microscope equipped with a Leitz Wetzlar Germany Type 307-148002 514687 mercury bulb and BP 340–380; BP 450–490 (for GFP visualizing); BP 515–560 filter sets. Images were obtained with a digital camera Axiocam Zeiss using AxioVision Rel. 4.8.2 Software.

Statistical analysis

All the data were collected from at least three independent experiments. For stopped-flow experiments, usually five runs at each temperature and ten runs for P_f at 23°C were stored and analyzed in each experiment. Student's t test was used for statistical analysis. $P<0.05$ (marked as *) was considered to be statistically significant. Data are presented as mean ± standard deviation (SD).

Results

Cloning and heterologous expression of *Vitis vinifera* aquaporins in *S. cerevisiae*

Specific primers designed from the sequences of aquaporins of *Vitis vinifera* (cv. Pinot Noir) were able to amplify six full-length cDNAs of putative aquaporins from *V. vinifera* (cv. Touriga nacional). The predicted amino acid sequences were aligned and compared with the Pinot noir variety (Figure S1), all of them shared high identity (>96%) in both varieties. As expected, the six amino acids sequences corresponding to the cDNAs cloned from *V. vinifera* cv. Touriga nacional in this study were clearly identified in the genome of Pinot noir variety and three of them were clustered in their subsequent groups of PIPs, while other three in TIPs subfamilies (Figure 1). Based on BLASTN (http://blast.ncbi.nlm.nih.gov/Blast.cgi) alignment, sequences were classified as *PIP1;4* (858 bp), *PIP2;1* (852 bp), *PIP2;3* (861 bp) and *TIP1;1* (753 bp), *TIP2;2* (750 bp), *TIP4;1* (759 bp) and their encoded proteins were named as *Vv*TnPIP1;4 (286 aa), *Vv*TnPIP2;1 (284 aa), *Vv*TnPIP2;3 (287 aa) and *Vv*TnTIP1;1 (251 aa), *Vv*TnTIP2;2 (250 aa), *Vv*TnTIP4;1 (253 aa) following the nomenclature proposed for plant aquaporins [30]. *Vv*TnPIP1;4 has 96.5% identity with nine substitution of amino acids (Figure S1A), while *Vv*TnPIP2;1 is 98.6% identical with difference at four positions (Figure S1B). *Vv*TnTIP2;2 shares 99.2% identity of amino acids with substitution at two positions (Figure S1C), similarly *Vv*TnTIP1;1 has 99.6% identity with substitution at only one amino acid position (Figure S1D). On the other hand, *Vv*TnPIP2;3 and *Vv*TnTIP4;1 were 100% identical to their respective proteins of the other variety (Figures S1E and S1F, respectively).

Expression and localization of these cloned proteins in selected yeast transformants were verified by GFP tagging under fluorescent microscopy. Most of the GFP-tagged aquaporins were localized in the plasma membrane of *S. cerevisiae* (Figure 2). Besides plasma membrane, some of the GFP-tagged proteins were also observed retained inside the cell, probably in the endoplasmic reticulum or vesicles of the secretory pathway.

Topology prediction and analysis of conserved sequences of *Vitis vinifera* aquaporins

The hypothetical transmembrane topology of deduced amino acid sequences revealed that, as expected, all cloned aquaporins exhibit typical features common to orthodox plant aquaporins (Figure 3): (i) six transmembrane-spanning hydrophobic α-helices (TMH1–TMH6) connected with five alternating extracellular and intracellular loops (LA-LE), (ii) intracellular facing amino and carboxyl terminals, (iii) two highly conserved NPA (Asn-Pro-Ala) motifs on LB and LE loops important for configuration of aqueous pore in aquaporins [31], and (iv) a Serine residue near the second NPA motif (GXXXNPAR(S/D)XG), specific for water transport [32,33].

Besides the general characteristics of aquaporins, special features attributed to the PIP aquaporin family and subfamilies (PIP1s and PIP2s) of *Vitis* aquaporins were found, such as: (i) longer N-terminal in *Vv*TnPIP1;4 (PIP1 subfamily) than *Vv*TnPIP2;1 and *Vv*TnPIP2;3 (PIP2 subfamily) (Figures 3 and S2A), (ii) longer C-terminal in *Vv*TnPIP2;1 and *Vv*TnPIP2;3 than *Vv*TnPIP1;4 [12,34] (Figures 3 and S2B), (iii) methylation site (K3/4 and E6) [35] and diacidic motif (D/E-I/X-E/D) [36] at N-terminal (*Vv*TnPIP1;4, *Vv*TnPIP2;1 and *Vv*TnPIP2;3) (Figures 3 and S3A), (iv) His residue for pH sensitivity in loop D (*Vv*TnPIP1;4-H^{206}, *Vv*TnPIP2;1-H^{196}, *Vv*TnPIP2;3-H^{199}) [37] (Figures 3 and S4B), (v) multiple conserved Ser residues for phosphorylation in loop B, loop D and C-terminal positions, such as 1) in loop B (*Vv*TnPIP1;4-S^{128}, *Vv*TnPIP2;1-S^{118} and *Vv*TnPIP2;3-S^{121}) (Figures 3 and S4A), 2) in loop D two positions of conserved Ser in consensus sequence N/SARDSHVP, in which the first Ser is present only in *Vv*TnPIP2;1 (S^{191}) [38], while second Ser is present in all cloned PIPs (*Vv*TnPIP1;4-S^{205},

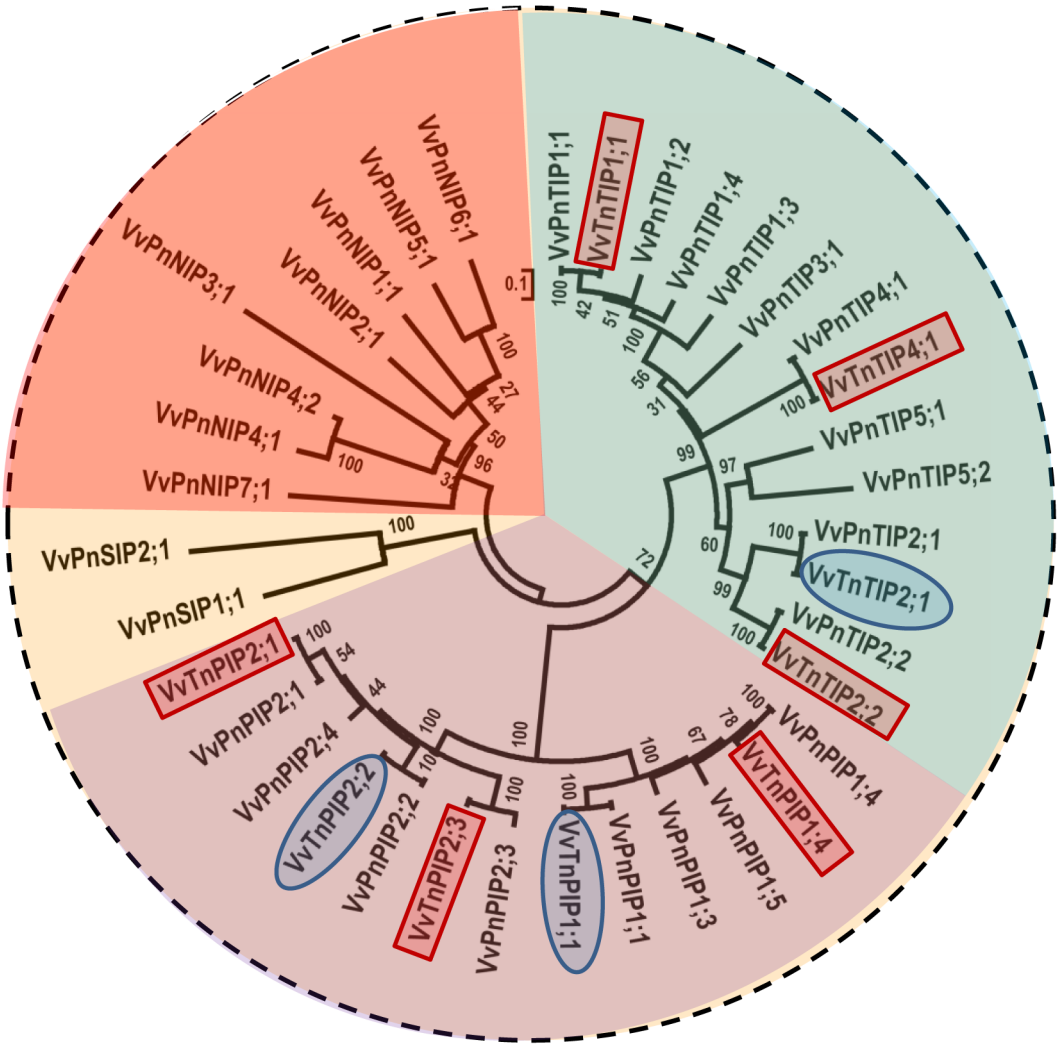

Figure 1. Phylogenetic tree based on protein sequences of aquaporins from *V. vinifera* cv. Pinot noir and cv. Touriga nacional. Dendrogram depicting the phylogenetic relationship between the aquaporins of Touriga nacional variety cloned in this study (framed in rectangular shape), previous study (oval shape frame) [17] with the aquaporins of Pinot noir variety. Dendogram was generated by neighbor-joining method (applied to 1000 bootstrap data sets) using the MEGA5.1 program [26]. Accession numbers of presented protein sequences are: *Vv*PnPIP1;1 (CAO41326, GSVIVT00029248001), *Vv*PnPIP1;3 (CAO62835, GSVIVT00000433001), *Vv*PnPIP1;4 (CAO39626, GSVIVT00026881001), *Vv*PnPIP1;5 (CAO39627, GSVIVT00026882001), *Vv*PnPIP2;1 (CAN75442), *Vv*PnPIP2;2 (CAO47394, GSVIVT00036133001), *Vv*PnPIP2;3 (CAO18152, GSVIVT00023192001), *Vv*PnPIP2;4 (CAO21844, GSVIVT00024536001), *Vv*PnTIP1;1 (CAO69259, GSVIVT00018548001), *Vv*PnTIP1;2 (CAO63006, GSVIVT00000605001), *Vv*PnTIP1;3 (CAO16745, GSVIVT00022146001), *Vv*PnTIP1;4 (CAO21720, GSVIVT00024394001), *Vv*PnTIP2;1 (CAO45860, GSVIVT00034350001), *Vv*PnTIP2;2 (CAO23095, GSVIVT00012703001), *Vv*PnTIP3;1 (CAO62035, GSVIVT00013854001), *Vv*PnTIP4;1 (CAO44039, GSVIVT00032441001), *Vv*PnTIP5;1 (CAO42713, GSVIVT00029946001), *Vv*PnTIP5;2 (CAO70596, GSVIVT00019170001), *Vv*PnNIP1;1 (CAO48005, GSVIVT00035815001), *Vv*PnNIP2;1 (CAO15462, GSVIVT00011149001), *Vv*PnNIP3;1 (CAO17108, GSVIVT00022377001), *Vv*PnNIP4;1 (CAO70192, GSVIVT00007127001), *Vv*PnNIP4;2 (CAO43338, GSVIVT00003903001), *Vv*PnNIP5;1 (CAO62847, GSVIVT00000446001), *Vv*PnNIP6;1 (CAO45476, GSVIVT00033750001), *Vv*PnNIP7;1 (CAO71103, GSVIVT00019910001), *Vv*PnSIP1;1 (CAO23510, GSVIVT00025504001) and *Vv*PnSIP2;1 (CAO18284, GSVIVT00023346001) (for Pinot noir cultivar sequences) and *Vv*TnPIP1;1 (HQ913643), *Vv*TnPIP1;4 (KJ697714), *Vv*TnPIP2;1 (KJ697715), *Vv*TnPIP2;2 (HQ913642), *Vv*TnPIP2;3 (KJ697716), *Vv*TnTIP1;1 (KJ697717), *Vv*TnTIP2;1 (HQ913640), *Vv*TnTIP2;2 (KJ697718) and *Vv*TnTIP4;1 (KJ697719) (for Touriga nacional cultivar sequences).
doi:10.1371/journal.pone.0102087.g001

*Vv*TnPIP2;1-S^{195} and *Vv*TnPIP2;3-S^{198}) [39] (Figures 3 and S4B), 3) at C-terminal, consensus phosphorylation site (Lys-x-x-x-Ser-x-Arg) is conserved only in PIP2 subfamily members (*Vv*TnPIP2;1-S^{277} and S^{280}, *Vv*TnPIP2;3-S^{280} and S^{283}) [40,41] (Figures 3 and S4C).

Distinct characteristics found in cloned TIPs were: (i) shorter N-terminals than PIPs (Figures 3 and S2A) (ii) slightly longer C-terminal than PIP1s, but shorter than PIP2s subfamily members (Figures 3 and S2B) [34] (iii) Cys residue for mercury sensitive site (*Vv*TnTIP1;1-C^{118}, *Vv*TnTIP2;2-C^{116} and *Vv*TnTIP4;1- C^{113}) [42] (Figures 3 and S5A), (iv) His residue for pH sensitive site (*Vv*TnTIP2;2-H^{131} and *Vv*TnTIP4;1-H^{128}) (Figures 3 and S5B) [17]. (viii) Thr residue for putative phosphorylation site (*Vv*TnTIP1;1-T^{99}, *Vv*TnTIP2;2-T^{97} and *Vv*TnTIP4;1-T^{94}) (Figures 3 and S4A) [40,43].

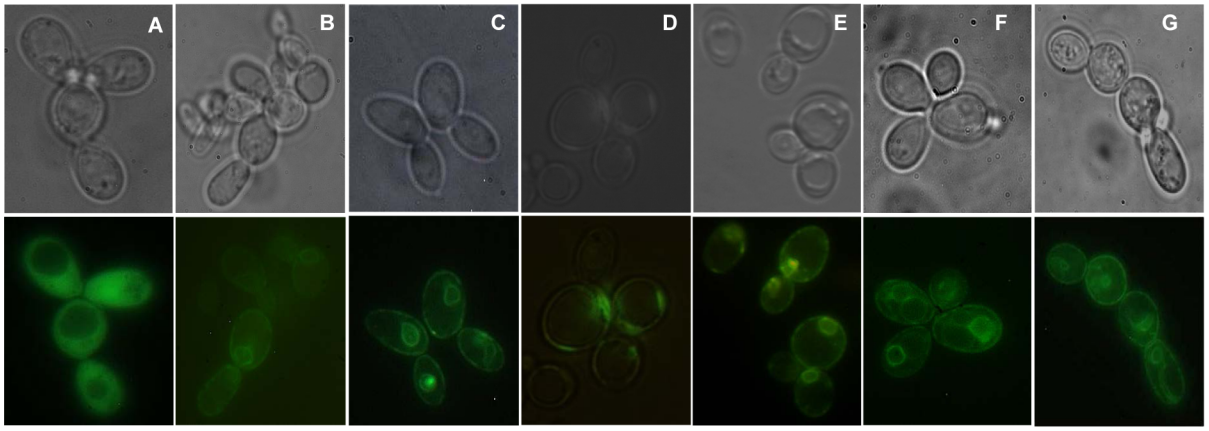

Figure 2. Localization of GFP-tagged aquaporins from *V. Vinifera* expressed in *S. cerevisiae* strains. Cytosolic GFP localization in (A) control cells (transformed with empty plasmid pUG35) and in the membrane of cells expressing (B) *Vv*TnPIP1;4, (C) *Vv*TnPIP2;1, (D) *Vv*TnPIP2;3, (E) *Vv*TnTIP1;1, (F) *Vv*TnTIP2;2, (G) *Vv*TnTIP4;1. Images were taken under phase contrast (upper panel) and fluorescence (lower panel) microscopy.
doi:10.1371/journal.pone.0102087.g002

Presence of signature sequences for transport of substrates other than water

Signature sequences for transport of atypical substrates in all cloned aquaporins were explored according to [4] (Table 1), in particular the ar/R (aromatic/Arginine) constriction (filter 2) that consists of four residues (one in the second and one in the fifth helix (TMH2 and TMH5) and two in the fifth loop (LE1 and LE2 or R)) and P1–P5 positions (P1 in the third loop (LC), P2 and P3 in the fifth loop (LE), P4 and P5 in sixth helix (TMH6)) (Figure 3). The analysis showed the presence of signature sequences deciphered for boron (filter 2: F/A/G-H/I/S-T/G/A-R and P1–P5 residues: Q/F/I-S/T-A-F/Y-W/L) (Figure S6A) and CO_2 (filter 2: F-H-T-R and P1–P5 residues: Q/M-S-A-F-W) (Figure S6B) transport in all cloned PIPs: *Vv*TnPIP1;4 (filter 2: F^{94}-H^{223}-T^{232}-R^{238} and P1–P5: Q^{154}-S^{239}-A^{243}-F^{258}-W^{259}), *Vv*TnPIP2;1 (filter 2: F^{84}-H^{213}-T^{222}-R^{228} and P1–P5: Q^{144}-S^{229}-A^{233}-F^{248}-W^{249}) and *Vv*TnPIP2;3 (filter 2: F^{87}-H^{216}-T^{225}-R^{231} and P1–P5: Q^{147}-S^{232}-A^{236}-F^{251}-W^{252}) (Table 1). Whereas, sequences for ammonia transport (filter 2: H/W-I/V-G/A-R and P1–P5 residues: T/F-S-A-Y-W/L) (Figure S7) were found in all the TIPs: *Vv*TnTIP1;1 (filter 2: H^{65}-I^{187}-A^{196}-V^{202} and P1–P5 residues: T^{125}-S^{203}-A^{207}-V^{219}-W^{220}), *Vv*TnTIP2;2 (filter 2: H^{63}-I^{185}-G^{194}-R^{200} and P1–P5 residues: T^{123}-S^{201}-A^{205}-V^{217}-W^{218} and *Vv*TnTIP4;1 (filter 2: H^{60}-V^{183}-A^{192}-R^{198} and P1–P5 residues: T^{120}-S^{199}-A^{203}-V^{215}-W^{216}) (Table 1). On the other hand, all cloned aquaporins exhibited the signature sequences for H_2O_2 transport (filter 2: H/F/W-I/H/V-A/T/G-R/V and P1–P5 residues: T/Q/F-S/A-A-Y/F-W/I) (Figure S8A) and urea transport (filter 2: F/H/G/A/N-I/H/S/V-T/A/G-R/V and P1–P5 residues: M/T/Q/L/F/V/I-S/A/T-A-F/Y-W/F/L) (Figure S8B) (Table 1).

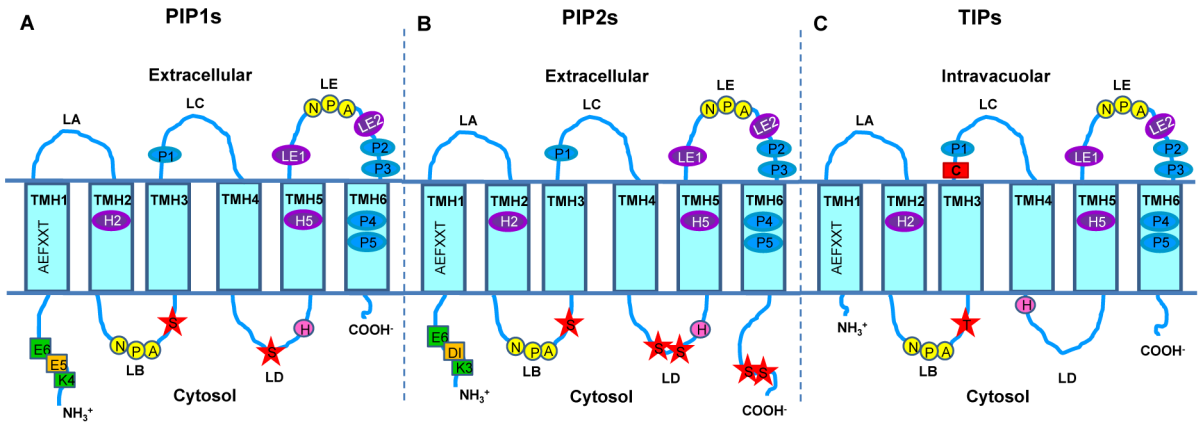

Figure 3. Schematic representation of predicted topology of *V. vinifera* aquaporins (PIP1s, PIP2s and TIPs) obtained in this study. These aquaporins consist of six transmembrane domains (TMH1–TMH6), five connecting loops (LA–LE) and N- and C-terminal extremities. The conserved NPA motifs (filter 1) are shown in yellow circles, while residues for ar/R constriction (filter 2) and P1–P5 positions for selectivity of atypical substrates (according to [4]) are shown in purple and blue ovals, respectively. Putative phosphorylation sites are marked as red stars, pH regulation sites are shown as pink rounds, green and yellow rectangles represent methylation and sorting signals. (A) PIP1s subfamily consisting of longer N-terminal with methylation and sorting signals, two putative phosphorylation sites in loop B and D, conserved His in loop D for pH regulation site and shorter C-terminal. (B) PIP2s subfamily having slightly shorter N-terminal with methylation and sorting signals conserved His in loop D for pH regulation, four Ser for putative phosphorylation: one in loop B, two in loop D and two in long C-terminal. (C) TIPs with very short N-terminal without sorting or methylation signals, only one conserved Thr residue instead of Ser residue for putative phosphorylation in loop B, Cys residue (red rectangle) in TMH4 for mercury sensitivity and His residue in loop D for pH regulation.
doi:10.1371/journal.pone.0102087.g003

Table 1. Specific amino acid residues for atypical substrates at ar/R constrictions and P1–P5 positions (based on [4]).

Aquaporins	Putative substrates	ar/R constrictions (filter 2)				P1–P5 positions				
		TMH2	TMH5	LE1	LE2	P1	P2	P3	P4	P5
*Vv*TnPIP1;4	Boron, CO_2, H_2O_2, urea	F^{94}	H^{223}	T^{232}	R^{238}	Q^{154}	S^{239}	A^{243}	F^{258}	W^{259}
*Vv*TnPIP2;1	Boron, CO_2, H_2O_2, urea	F^{84}	H^{213}	T^{222}	R^{228}	Q^{144}	S^{229}	A^{233}	F^{248}	W^{249}
*Vv*TnPIP2;3	Boron, CO_2, H_2O_2, urea	F^{87}	H^{216}	T^{225}	R^{231}	Q^{147}	S^{232}	A^{236}	F^{251}	W^{252}
*Vv*TnTIP1;1	Urea, NH_3, H_2O_2	H^{65}	I^{187}	A^{196}	V^{202}	T^{125}	S^{203}	A^{207}	V^{219}	W^{220}
*Vv*TnTIP2;2	Urea, NH_3, H_2O_2	H^{63}	I^{185}	G^{194}	R^{200}	T^{123}	S^{201}	A^{205}	V^{217}	W^{218}
*Vv*TnTIP4;1	Urea, NH_3, H_2O_2	H^{60}	V^{183}	A^{192}	R^{198}	T^{120}	S^{199}	A^{203}	V^{215}	W^{216}

doi:10.1371/journal.pone.0102087.t001

Functional characterization of water transport in yeast strains expressing *V. vinifera* aquaporins

Water transport activity of heterologously expressed *Vitis* aquaporins in yeast strains was assayed by stopped-flow fluorescence spectroscopy. The shrinking rate of yeast cells upon a sorbitol hyperosmotic shock was monitored as change in fluorescence signals (Figure 4A). The strain with empty plasmid (pUG35), devoid of water channels, was used as control ($P_f = 4.30 \pm 0.28 \times 10^{-4}$ cm s^{-1}). Water permeability (P_f) of yeast cells was not affected by the expression of *Vv*TnPIP1;4 ($4.0 \pm 0.35 \times 10^{-4}$ cm s^{-1}), *Vv*TnPIP2;3 ($5.30 \pm 0.63 \times 10^{-4}$ cm s^{-1}) and *Vv*TnTIP4;1 ($3.3 \pm 0.08 \times 10^{-4}$ cm s^{-1}) (Table 2, Figure 4B). Thus, these strains were considered as non-functional for water transport. On the other hand, heterologous expression of *Vv*TnPIP2;1 ($7.43 \pm 0.64 \times 10^{-4}$ cm s^{-1}), *Vv*TnTIP1;1 ($8.06 \pm 0.34 \times 10^{-4}$ cm s^{-1}) and *Vv*TnTIP2;2 ($9.65 \pm 0.026 \times 10^{-4}$ cm s^{-1}) (Table 2, Figure 4B) led to 73%, 88% and 125%, respectively, higher water permeability and were stated as functional for water transport. Among all cloned *Vitis* aquaporins, TIPs (*Vv*TnTIP1;1, *Vv*TnTIP2;2) exhibited higher water conductivity as compared to *Vv*TnPIP2;1.

To evaluate the activation energy for water transport, P_f values of all yeast strains were analyzed in a range of temperatures (9–37°C) and Arrhenius plots were drawn (Figure 5A). As expected, transport of water was strongly dependent on temperature in control yeast strain, as reflected by higher activation energy *Ea* (14.05 ± 0.01 kcal mol^{-1}) (Figure 5B and Table 2). Arrhenius plots for *Vv*TnPIP1;4, *Vv*TnPIP2;3 and *Vv*TnTIP4;1 expressing yeast strains exhibited parallel steep slopes, overlapped with control strain (Figure 5A) and almost similar activation energies (14.74 ± 0.62, 14.53 ± 0.55, 14.86 ± 0.22 kcal mol^{-1}, respectively) (Figure 5B and Table 2). On the other hand, expression of *Vv*TnPIP2;1, *Vv*TnTIP1;1 and *Vv*TnTIP2;2 led to drastic reduction in the activation energies to 10.84 ± 0.83, 8.8 ± 0.77 and 8.77 ± 0.62 kcal mol^{-1}, respectively (Figure 5B and Table 2), demonstrating that transport of water was majorly mediated by aquaporins in these yeast strains.

To examine the dose and time dependent effects of mercurial inhibition, yeast strains expressing functional *Vitis* aquaporins (*Vv*TnPIP2;1, *Vv*TnTIP1;1 and *Vv*TnTIP2;2) as well as the control strain were pretreated with various concentrations (0.5 and 1.0 mM) of $HgCl_2$ for 15 to 30 minutes at room temperature, before hyperosmotic shock. Figure 6A compares the stopped-flow signals of yeast cells expressing *Vv*TnTIP2;2, obtained after hyperosmotic shock either in the absence or presence of mercury chloride (0.5 mM) after 15 minutes of incubation. It is clear from the signals that $HgCl_2$ reduced the shrinking rates of the cells. All the functional aquaporins tested were mercury sensitive. TIPs were more sensitive than PIP. P_f was markedly decreased when cells were incubated with 0.5 mM $HgCl_2$ for 15 minutes before the osmotic shock. P_f of *Vv*TnPIP2;1 expressing strain was reduced by 24% while *Vv*TnTIP1;1 and *Vv*TnTIP2;2 expressing strains exhibited 38% and 36% reduction (Figure 6B). Water transport in control cells was not affected by 0.5 mM $HgCl_2$, even after 30 minutes of incubation, while higher concentration (1 mM) reduced the P_f of all yeast strains including the control strain, indicating a general toxicity at this concentration (data not shown).

Growth assays under osmotic stress and in the presence of atypical substrates

Expression of *Vitis* aquaporins in *S. cerevisiae* was not deleterious to yeast cells, since neither the specific growth rate nor the final biomass of the yeast were affected during growth in standard YNB media. Accordingly, all the strains showed

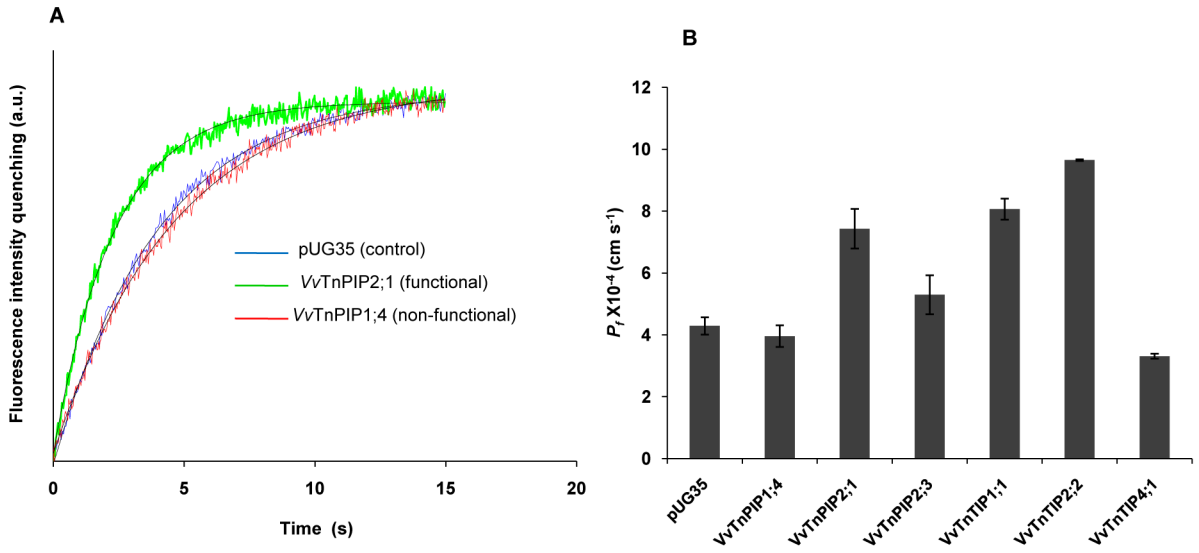

Figure 4. Stopped-flow assays for measurement of water transport activity of *V. vinifera* aquaporins expressed in yeast. (A) Typical traces obtained from stopped-flow spectroscopy after hyperosmotic shock. Presented signals are illustrative of ten traces at 23°C obtained from strains expressing functional (*Vv*TnPIP2;1) and non-functional (*Vv*TnTIP4;1) aquaporins for water transport, and control (transformed with empty plasmid pUG35). (B) Water permeability coefficients (P_f at 23°C) of *Vv*TnPIP2;1, *Vv*TnTIP1;1 and *Vv*TnTIP2;2 were higher than control strain. Expression of *Vv*TnPIP1;4, *Vv*TnPIP2;3 and *Vv*TnTIP4;1 did not increase water permeability in yeast cells. Data are mean ± SD of three independent experiments with at least ten traces.
doi:10.1371/journal.pone.0102087.g004

approximately 3.5 hours of doubling time and grew up to similar final biomass in liquid YNB media (data not shown).

Expression of Vitis aquaporins affects the growth of yeast cells under osmotic stress. Osmotic tolerance/susceptibility of heterologously expressed *Vitis* aquaporins was examined in the presence of NaCl, KCl and sorbitol. When exposed to hyperosmotic stress, yeast cells expressing *Vitis* aquaporins exhibited decreased growth to a variable degree, depending on the types of aquaporins expressed (Figure 7). Growth of all yeast strains (including empty plasmid strain) was equally inhibited in the presence of NaCl, even at lower concentration (0.5 M) (data not shown). At the highest concentration of KCl (1.5 M), cells expressing *Vv*TnTIP4;1 were least inhibited by KCl, while growth of *Vv*TnTIP2;2 and *Vv*TnPIP1;4 expressing cells displayed a clear osmosensitive phenotype followed by *Vv*TnTIP1;1, *Vv*TnPIP2;3 and *Vv*TnPIP2;1 (Figure 7). Growth of these strains was reduced under osmoequivalent concentration of sorbitol (2.1 M), but did not show any clear phenotype (Figure 7).

Expression of *V. vinifera* aquaporins increases the sensitivity of yeast to H_2O_2 and boron. Ability of *Vitis* aquaporins to facilitate the transport of H_2O_2 and boron was examined by drop test assays in the presence of these substrates on solid YNB (pH 5.0). Impaired growth of yeast strains due to the expression *Vitis* aquaporins was tested in the presence of these substrates.

Growth of *Vitis* aquaporins (*Vv*TnPIP1;4, *Vv*TnPIP2;1, *Vv*TnPIP2;3, *Vv*TnTIP1;1 and *Vv*TnTIP2;2) expressing strains was affected by externally supplied H_2O_2 in a dose dependent manner (Figure 8). Impaired growth of *Vitis* aquaporins expressing strains was observed at higher concentration of H_2O_2 (0.75 mM) (Figure 8), while the control strain was able to grow up to the last dilution at 1.0 mM H_2O_2. Growth of the strain expressing *Vv*TnTIP2;2 was most severely inhibited, followed by *Vv*TnTIP1;1, *Vv*TnPIP2;3, *Vv*TnPIP1;4 and *Vv*TnPIP2;1 expressing strains (Figure 8). Cells expressing *Vv*TnTIP4;1 were least sensitive toward H_2O_2 and exhibited similar growth as the control strain.

The ability of *Vitis* aquaporins to facilitate boron transport was tested in the same way as H_2O_2. Yeast transformants were spotted

Table 2. Water transport activity in *V. vinifera* aquaporins expressed in *S. cerevisiae*.

Yeast strains expressing *Vitis* aquaporins	Permeability coefficient (P_f) (cm s^{-1})×10^{-4}	Activation energy (*Ea*) (kcal mol^{-1})
pUG35	4.3±0.28	14.05±0.01
*Vv*TnPIP1;4	4.0±0.35	14.74±0.62
*Vv*TnPIP2;1	7.43±0.64	10.84±0.83
*Vv*TnPIP2;3	5.30±0.63	14.53±0.55
*Vv*TnTIP1;1	8.06±0.34	8.79±0.77
*Vv*TnTIP2;2	9.65±0.03	8.77±0.62
*Vv*TnTIP4;1	3.31±0.08	14.86±0.22

Data are mean ± SD of three independent experiments with at least ten traces.
doi:10.1371/journal.pone.0102087.t002

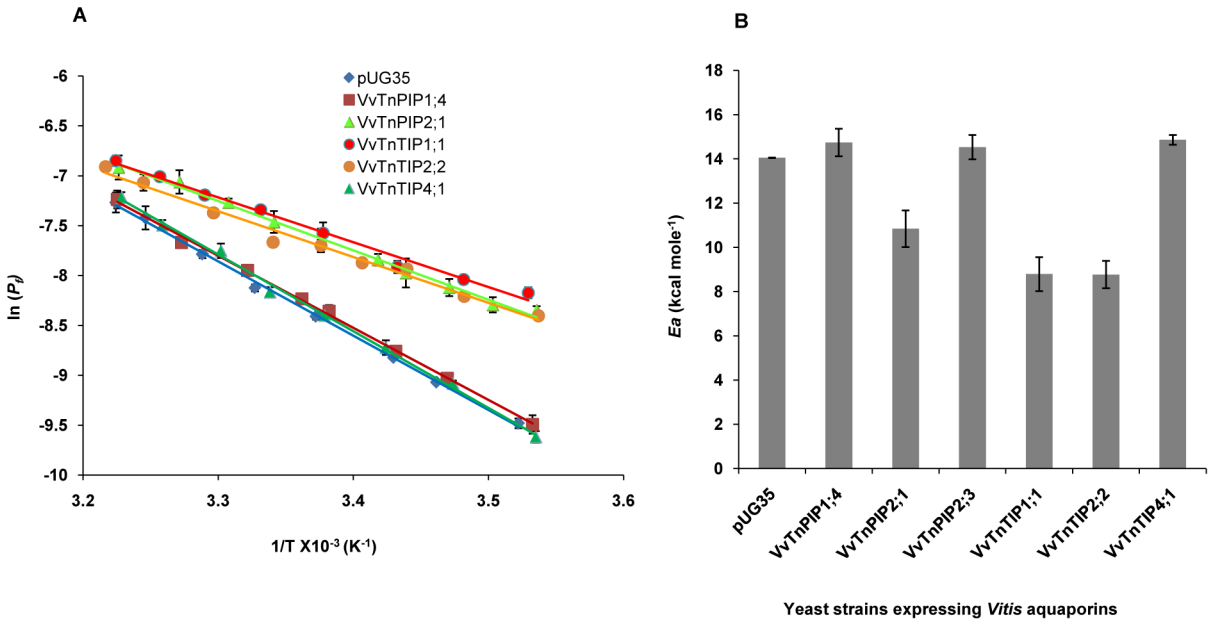

Figure 5. Activation energies (*Ea*) of water transport in *V. vinifera* aquaporins expressed in yeast. (A) Arrhenius plot of P_f at temperature range (9–37°C), where T is temperature in Kelvin. *Ea* was evaluated from the slopes. Strains expressing *Vv*TnPIP1;4, *Vv*TnTIP4;1 and empty plasmid (pUG35) showed steeper slope, while strains expressing *Vv*TnPIP2;1, *Vv*TnTIP1;1 and *Vv*TnTIP2;2 exhibited shallow slope. (B) Calculated *Ea* from the slope showed that *Vv*TnPIP2;1, *Vv*TnTIP1;1 and *Vv*TnTIP2;2 expressing strains exhibited lower *Ea*, while *Vv*TnPIP1;4, *Vv*TnPIP2;3 and *Vv*TnTIP4;1 expressing strains showed were almost equal to control strain (pUG35). Data are mean ± SD of three independent experiments with at least five traces (ten traces in case of P_f at 23°C) at each temperature.
doi:10.1371/journal.pone.0102087.g005

on YNB plates containing various concentrations of boron as boric acid (Figure 9). The exposure to boric acid (40 mM) caused reduced growth of strains expressing *Vitis* aquaporin. Interestingly, at 40 mM boric acid, cells transformed with *Vv*TnTIP4;1 grew better in comparison to control strain, but these cells showed clear sensitivity toward boric acid when exposed to higher concentration (60 mM) of boric acid. Heterologous expression of all cloned *Vitis* aquaporins, except *Vv*TnPIP2;1, showed increased sensitivity to 60 mM boric acid. *Vv*TnPIP2;1 expressing strain was the most tolerant to externally supplied boric acid and was able to grow as the control strain. Growth of *Vv*TnTIP2;2 expressing strain was severely inhibited by boric acid exposure (Figure 9).

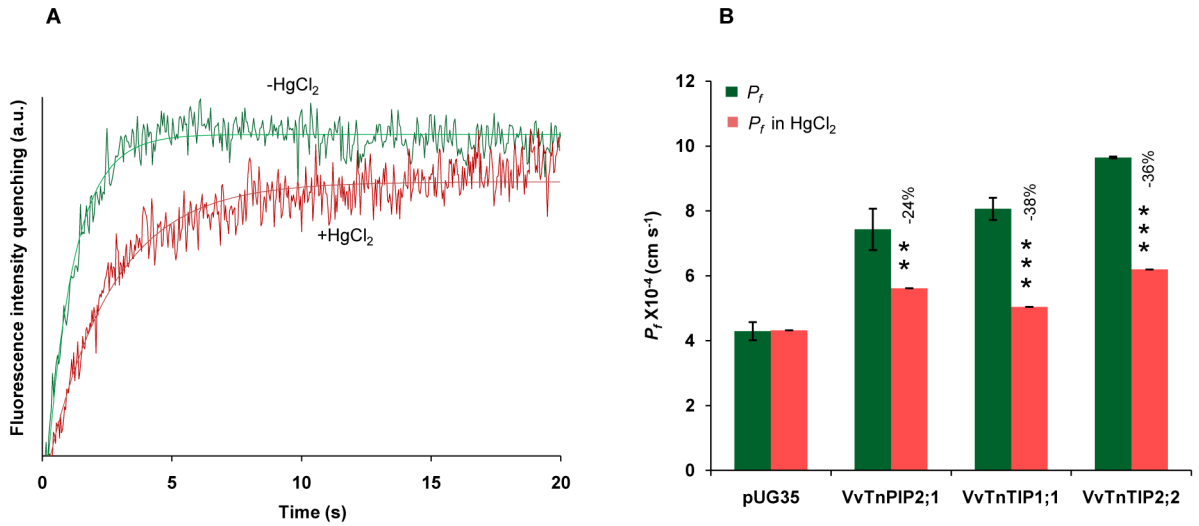

Figure 6. Inhibition of water permeability by mercury chloride ($HgCl_2$) in yeast strains expressing *V. vinifera* aquaporins. (A) Inhibition of water permeability in yeast cells expressing functional aquaporin (*Vv*TnTIP2;2) by $HgCl_2$. The green signal represents water permeability without $HgCl_2$ and the red signal shows the lower permeability when cells were incubated with 0.5 mM $HgCl_2$ for 15 minutes prior to osmotic shock. (B) Water permeability coefficients (P_f at 23°C) of *Vv*TnPIP2;1, *Vv*TnTIP1;1 and *Vv*TnTIP2;2 were reduced by 0.5 mM $HgCl_2$. Data are mean ± SD of three independent experiments with at least five traces. The data were analyzed by *t-test* and asterisks above bars indicate statistically significant differences, where **p<0.01, ***p<0.001.
doi:10.1371/journal.pone.0102087.g006

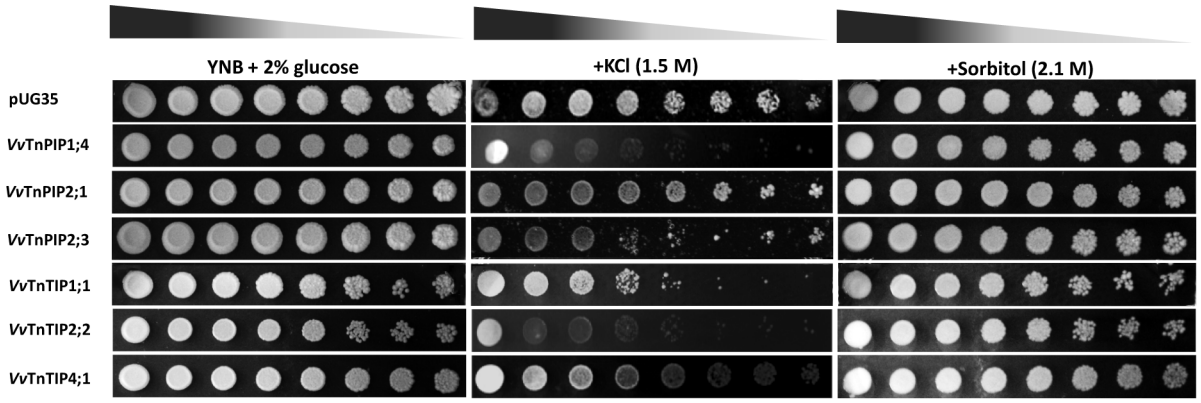

Figure 7. Growth assays of *S. cerevisiae* strains expressing *V. vinifera* aquaporins under osmotic stress. Hyperosmotic stress was exerted by osmo-equivalent concentration of either KCl or sorbitol. Yeast strain transformed with empty pUG35 plasmid was used as control (pUG35). Yeast suspensions were spotted in 10-fold dilution on solid YNB plates without or with 1.5 M KCl or 2.1 M sorbitol. Growth was recorded after two weeks at 28°C. Photographs shown are representative of three independent experiments with consistent results.
doi:10.1371/journal.pone.0102087.g007

We also performed the growth assays of yeast strains expressing *Vitis* aquaporins in the presence of ammonia and urea, to explore their possible transport by aquaporins. We observed that growth of yeast strains was not affected by these substrates at any tested concentrations, since no distinct growth phenotypes were observed (results not shown).

Discussion

In this study we have cloned and characterized three plasma membrane (PIPs) and three tonoplast (TIPs) aquaporins from *Vitis vinifera* cv. Touriga nacional, an important Portuguese cultivar, widely believed to produce the finest red wines of Portugal.

All the cloned full length aquaporin genes from *V. vinifera* (cv. Touriga nacional) encoding three PIPs (*Vv*TnPIP1;4, *Vv*TnPIP2;1 and *Vv*TnPIP2;3) and TIPs (*Vv*TnTIP1;1, *Vv*TnTIP2;2 and *Vv*TnTIP4;1) proteins showed obvious similarity with the same proteins of the database variety of *V. vinifera* (cv. Pinot noir). Their plasma membrane localization was confirmed by GFP-tagging, although we observed a partial retention in intracellular structures, probably in endoplasmic reticulum or in vesicles of secretory pathway (reviewed by [6]). Several reports suggest that a fraction of intracellular plant aquaporins (TIPs) is generally "miss-targeted" to the plasma membrane of heterologous models, which enabled the researchers to measure their water transport activity in *Xenopus* and yeast (reviewed by [44]).

Their sequence analysis for topological prediction revealed all the characteristics of typical aquaporin subfamilies. Specific residues for transport of ammonia (filter 2: H/W-I/V-G/A-R and P1–P5 residues: T/F-S-A-Y-W/L), boron (filter 2: F/A/G-H/I/S-T/G/A-R and P1–P5 residues: Q/F/I-S/T-A-F/Y-W/L), CO_2 (filter 2: F-H-T-R and P1–P5 residues: Q/M-S-A-F-W), H_2O_2 (filter 2: H/F/W-I/H/V-A/T/G-R/V and P1–P5 residues: T/Q/F-S/A-A-Y/F-W/I) and urea (filter 2: F/H/G/A/N-I/H/S/V-T/A/G-R/V and P1–P5 residues: M/T/Q/L/F/V/I-S/A/T-A-F/Y-W/F/L) were present at ar/R constriction and P1–P5 positions [4] of the cloned *Vitis* aquaporins, depending on their subfamilies (Table 1).

Expression of functional aquaporins *Vv*TnPIP2;1, *Vv*TnTIP1;1 and *Vv*TnTIP2;2 increased the water permeability coefficient (P_f) and reduced the activation energy (*Ea*) required for water transport in yeast cells, while expression of non-functional aquaporins *Vv*TnPIP1;4, *Vv*TnPIP2;3 and *Vv*TnTIP4;1 expression exhibited higher *Ea* and did not affect P_f. The obtained

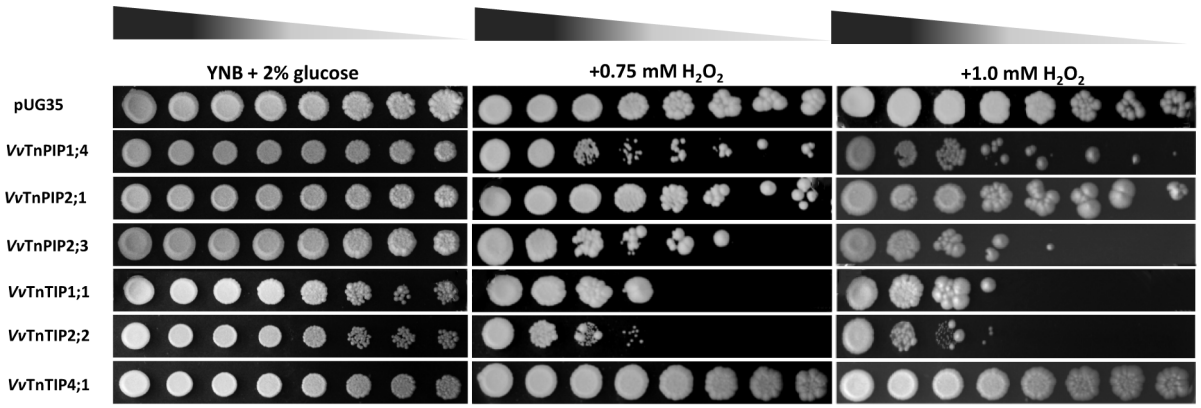

Figure 8. Growth assays of *S. cerevisiae* strains expressing *V. vinifera* aquaporins on H_2O_2 containing minimal media. Yeast strain transformed with empty pUG35 plasmid was used as control (pUG35). Yeast suspensions were spotted in 10-fold dilution on solid YNB plates without or with 0.75 mM and 1.0 mM H_2O_2. Growth was recorded after two weeks at 28°C. Photographs shown are representative of three independent experiments with consistent results.
doi:10.1371/journal.pone.0102087.g008

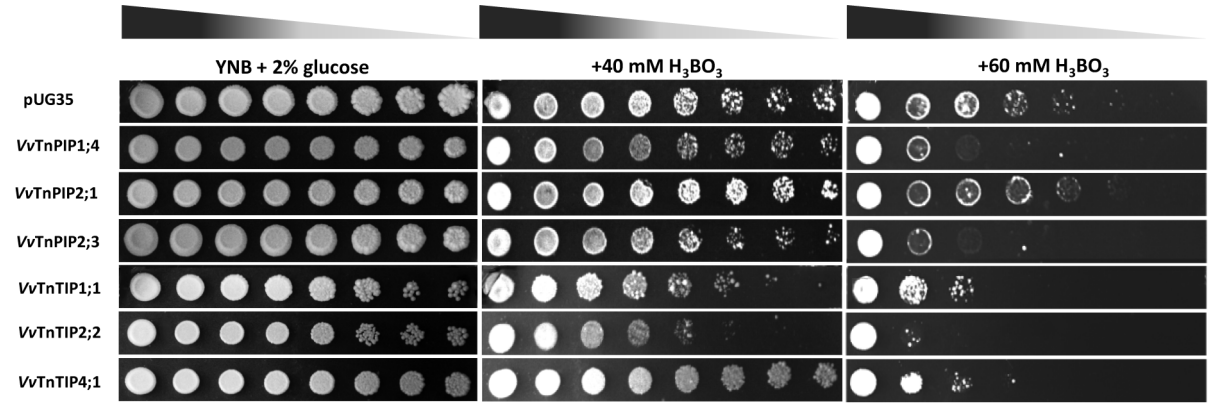

Figure 9. Growth assays of *S. cerevisiae* strains expressing *V. Vinifera* aquaporins on minimal medium containing boric acid. Yeast strain transformed with empty pUG35 plasmid was the control (pUG35). Yeast suspensions were spotted in 10-fold dilution on solid YNB plates without or with 40 mM and 60 mM boric acid. Growth was recorded after two weeks at 28°C. Photographs shown are representative of three independent experiments with consistent results.
doi:10.1371/journal.pone.0102087.g009

higher *Ea* and lower P_f can not be correlated with their lower plasma membrane expression since all the functional aquaporins were also partially retained at various subcellular regions and, on the other hand, one of the aquaporins (*Vv*TnTIP4;1) showed to be localized at the plasma membrane of *S. cerevisiae* and exhibited low water transport.

TIPs (*Vv*TnTIP1;1 and *Vv*TnTIP2;2) exhibited higher water conductivity in comparison to PIP (*Vv*TnPIP2;1). This finding is in agreement with previous reports of heterologously expressed plant aquaporins [41,45,46]. Higher water permeability of TIPs may be required for the central role of vacuole in osmoregulation of the cytoplasm. Constitutively higher water permeability of tonoplast aquaporins may allow the cells to use the vacuolar space to maintain the cellular integrity, in case of osmotic fluctuations caused by rapid water exchange during stress or developmental stages of plants (reviewed in [43,45]).

All functional *Vitis* aquaporins were found to be mercury-sensitive, as their P_f was reduced by mercury chloride. Many plant aquaporins have been inhibited by mercurial reagents, which bind to a conserved cysteine residue located downstream to first NPA motif, subsequently blocking the pore and shutting-down the aqueous pathway (reviewed in [3]). Notably all cloned TIPs showed the conserved cysteine residue responsible for mercury sensitivity (Figure S5A). Although PIPs (except *Vv*TnPIP2;3) did not have the conserved cysteine at the same position of alignment, they have four conserved cysteine residues in second and third transmembrane helices and one of these residues may represent the mercury sensitive site [47].

Transport of solutes of physiological significance, such as CO_2, H_2O_2, boron or silicic acid is now well established and has linked aquaporins to many functions, including carbon metabolism, oxidative stress responses, and plant mineral nutrition [3]. We performed a broad screening of growth sensitivity test of all cloned *Vitis* aquaporins on H_2O_2 and boric acid containing plates to investigate their ability to transport these atypical substrates. The phenotypic growth variations showed that heterologous expression of all cloned *Vitis* aquaporins (except *Vv*TnTIP4;1) caused more susceptibility to externally applied H_2O_2, indicating their putative role in H_2O_2 transport. In principle, increased level of H_2O_2 can disturb the cellular metabolism in an unidentified manner, which may lead to reduced or impaired growth of yeast cells. A higher permeability of H_2O_2 by heterologously expressed aquaporins might have increased the influx of H_2O_2 into yeast cells and eventually triggered the cell death or growth inhibition. H_2O_2, a long-lived reactive oxygen species (ROS) shares molecular properties with water, it can form hydrogen bonds and has similar permeability as water [48,49]. Based on the sensitivity of yeast cells expressing *Vitis* aquaporins, we assume that both *Vitis* PIPs and TIPs may permeate H_2O_2. Similar results were previously reported in heterologously expressed *Arabidopsis* [50–52] and maize aquaporins [53] expressed in *S. cerevisiae*. It is noteworthy that putative amino acids for H_2O_2 transport were found at ar/R constriction of all cloned *Vitis* aquaporins. Besides a potential threat to biological components, H_2O_2 also acts as a physiologically important molecule to activate Ca^{2+} channels for NADPH oxidase activity required during root hair growth and stomatal movement [54]. Under stress, H_2O_2 can be compartmentalized in various intracellular organelles as well as outside of the cells in apoplastic regions [55]. Further, the extracellular accumulated H_2O_2 can act as a regulator of water homeostasis by triggering the PIP internalization in *Arabidopsis* roots and consequently reduces the water permeability in roots under stress [56]. The role of *Vitis* PIPs may be involved in apoplastic exclusion of excess H_2O_2. Our results indicate that not only plasma membrane aquaporins (PIPs), but also tonoplast aquaporins (TIPs) are involved in H_2O_2 transport. Results of growth assays suggest that the cells expressing TIPs were more sensitive as compared with the cells expressing PIPs. TIPs are reported to be more diverse transporters and can conduct many solutes other than water due to having relatively weak selectivity (reviewed in [52,57]). Under elevated stress conditions, plant TIPs are suggested to transport high amounts of H_2O_2 into vacuoles, resulting in their further detoxification by vacuolar peroxidases using vacuole stored flavanoids as an electron donors [50]. Expression level of TIPs was found to be affected by H_2O_2 in tulip flowers [58] and it was suggested that TIPs triggered the ROS translocation into the vacuoles for their detoxification [57].

When exposed to H_2O_2, all yeast cells exhibited fluffy and larger colony morphology with rough edges (results not shown). H_2O_2 induces aging of the cells by releasing free radicals, leading to higher number of old cells which are bigger in size in comparison to young cells and eventually make the larger colonies with mature

cells [59]. Fluffy and rough surface colonies may represent a metabolic strategy of growth under unfavorable conditions [60].

Growth assays in the presence of boric acid showed that strains expressing *Vitis* aquaporins were more sensitive in comparison to control strain. Heterologous expression of plant aquaporins either in *Xenopus laevis* oocytes or *S. cerevisiae*, suggests that besides other routes, boron can be transported through PIPs [61,62] and NIPs [63–66]. NIP5;1 and NIP6;1 of *Arabidopsis thaliana* were identified as boric acid channels and were up-regulated under limited boron supply to accomplish the demand of boric acid [63,64]. Although boron is an essential micronutrient for plants, when accumulated at higher concentration it leads to toxicity. Being a non-charged molecule, boric acid can passively diffuse across lipid bilayer, but only significantly at high concentration gradient caused by high boron supply [67]. In plants, urea (*DUR3*) and glycerol (*FPS1*) transporters were identified as boron importers, while *BOR1* and its homolog *ScBOR1* of *S. cerevisiae* were characterized as boron exporters, exporting boron and protecting the cells from boron toxicity [68]. In this work, all the yeast strains expressing *Vitis* aquaporins have the same background for passive diffusion or importers and exporters of boric acid in their native membrane. Since different levels of toxicity were detected (Figure 9), we can speculate the putative transport of boron by *Vitis* aquaporins resulting in growth inhibition. Similarly, heterologously expressed barley *Hv*NIP2;1 [66], *Hv*PIP1;3 and *Hv*PIP1;4 [62] displayed sensitive growth phenotype in the presence of boron and were identified as boron transporters. Interestingly, all PIPs exhibited the signature sequences for boron transport and showed sensitivity (except *Vv*TnPI2;1) to boric acid. On the contrary, these conserved residues were not present in TIPs, although yeast strains expressing TIPs also exhibited increased sensitivity toward boron.

Although these studies are based on the molecular analysis of ar/R regions of *Vitis* aquaporins and indirect yeast based sensitivity growth assays on these substrates, transport of H_2O_2 and boron by *Vitis* aquaporins can be hypothesized.

In conclusion, we have cloned six PIPs and TIPs aquaporins from grapevine (cv. Touriga nacional) in *S. cerevisiae*, and have shown that three of them facilitate the transport of water. Reduced growth and survival of *Vitis* aquaporins expressing yeast cells in the presence of H_2O_2 and boron, indicates their probable role in transport of these non-aqua substrates. Additionally, expression of three aquaporins in yeast, which were found non-functional for water transport, exhibited sensitive phenotype when grown in the presence of these substrates, suggests their possible role in transport of substrates other than water. The combined use of molecular analysis of their sequences and functional investigation of growth sensitivity assays provided the initial insight on the selectivity profiles of *Vitis* aquaporins. Further studies are required to ascertain the role of *Vitis* aquaporins in transport of H_2O_2 and boron. Moreover, co-expression of aquaporins in *S. cerevisiae* may represent the next step for better understanding their interaction and regulation in plants.

Supporting Information

Figure S1 Comparison of *V. vinifera* aquaporins from Pinot noir and Touriga nacional cultivars. Alignment of deduced amino acid sequences of *Vv*TnPIP1;4 (A), *Vv*TnPIP2;1 (B), *Vv*TnPIP2;3 (C), *Vv*TnTIP1;1 (D), *Vv*TnTIP2;2 (E), *Vv*TnTIP4;1 (F) obtained from the present study (Touriga nacional) with the database variety (Pinot noir). Accession numbers of presented protein sequences are: *Vv*PnPIP1;4 (CAO39626), *Vv*TnPIP1;4 (KJ697714), *Vv*PnPIP2;1 (CAN75442), *Vv*TnPIP2;1 (KJ697715), *Vv*PnPIP2;3 (CAO18152), *Vv*TnPIP2;3 (KJ697716), *Vv*PnTIP1;1 (CAO69259), *Vv*TnTIP1;1 (KJ697717), *Vv*PnTIP2;2 (CAO23095), *Vv*TnTIP2;2 (KJ697718), *Vv*PnTIP4;1 (CAO44039), *Vv*TnTIP4;1 (KJ697719).
(PDF)

Figure S2 Comparison of N- (A) and C- (B) terminals of PIP1s, PIP2s and TIPs aquaporins. Aquaporins cloned in the present study are marked with red arrows. Accession numbers of presented protein sequences are: *At*PIP2;1 (P43286), *At*-deltaTIP2 (CAB10515), *At*-gammaTIP3 (AAC62778), *At*-epsilon-TIP (AAC42249), *Fa*PIP2;1 (ADJ67992), *Pv*-alphaTIP (CAA44669), *So*PIP2;1 (4JC6_N), *Vv*PnPIP1;1 (CAO41326), *Vv*TnPIP1;1 (HQ913643), *Vv*PnPIP1;4 (CAO39626), *Vv*TnPIP1;4 (KJ697714), *Vv*PnPIP2;1 (CAN75442), *Vv*TnPIP2;1 (KJ697715), *Vv*PnPIP2;2 (CAO47394), *Vv*TnPIP2;2 (HQ913642), *Vv*PnPIP2;3 (CAO18152), *Vv*TnPIP2;3 (KJ697716), *Vv*PnTIP1;1 (CAO69259), *Vv*TnTIP1;1 (KJ697717), *Vv*PnTIP2;1 (CAO45860), *Vv*TnTIP2;1 (HQ913640), *Vv*PnTIP2;2 (CAO23095), *Vv*TnTIP2;2 (KJ697718), *Vv*PnTIP4;1 (CAO44039), *Vv*TnTIP4;1 (KJ697719), *Zm*PIP2;1 (Q84RL7), *Zm*PIP2;5 (Q9XF58). *At*: *Arabidopsis thaliana*, *Fa*: *Fragaria*×*ananassa*, *Pv*: *Phaseolus vulgaris*, *So*: *Spinacia oleracea*, *Vv*Pn: *Vitis vinifera* cv. Pinot noir, *Vv*Tn: *V. vinifera* cv. Touriga nacional.
(PDF)

Figure S3 Presence of methylation and sorting signal sequences (D/E-X-D/E) at N-terminal (A) and pH regulation site (His residue) for gating (B) of PIPs aquaporins. Consensus sequences are framed and conserved residues are indicated as red triangle. Aquaporins cloned in the present study are marked with red arrows. Accession numbers of presented protein sequences are: *At*PIP2;1 (P43286), *At*PIP1;2 (Q06611), *At*PIP1;4 (Q39196), *Fa*PIP2;1 (ADJ67992), *So*PIP2;1 (4JC6_N), *Vv*PnPIP1;1 (CAO41326), *Vv*TnPIP1;1 (HQ913643), *Vv*PnPIP1;4 (CAO39626), *Vv*TnPIP1;4 (KJ697714), *Vv*PnPIP2;1 (CAN75442), *Vv*TnPIP2;1 (KJ697715), *Vv*PnPIP2;2 (CAO47394), *Vv*TnPIP2;2 (HQ913642), *Vv*PnPIP2;3 (CAO18152), *Vv*TnPIP2;3 (KJ697716), *Zm*PIP2;1 (Q84RL7), *Zm*PIP2;5 (Q9XF58), *Zm*PIP2;4 (Q9ATM6). *At*: *Arabidopsis thaliana*, *Fa*: *Fragaria*×*ananassa*, So: *Spinacia oleracea*, *Vv*Pn: *Vitis vinifera* cv. Pinot noir, *Vv*Tn: *V. vinifera* cv. Touriga nacional, *Zm*: *Zea mays*.
(PDF)

Figure S4 Putative phosphorylation sites in aquaporins. Ser residue in PIPs and Thr residue in TIPs aquaporins in loop B (A), loop D (B) and C-terminal (C) are tentative phosphorylation sites. Consensus sequences are framed and conserved residues are indicated as red triangle. Aquaporins cloned in the present study are marked with red arrows. Accession numbers of presented protein sequences are: *At*PIP1;2 (Q06611), *At*PIP1;4 (Q39196), *At*PIP2;1 (P43286), *At*-deltaTIP2 (CAB10515), *At*-gammaTIP3 (AAC62778), *At*-alphaTIP (AAC42249), *Fa*PIP2;1 (ADJ67992), *So*PIP2;1 (4JC6_N), *Vv*PnPIP1;1 (CAO41326), *Vv*TnPIP1;1 (HQ913643), *Vv*PnPIP1;4 (CAO39626), *Vv*TnPIP1;4 (KJ697714), *Vv*PnPIP2;1 (CAN75442), *Vv*TnPIP2;1 (KJ697715), *Vv*PnPIP2;2 (CAO47394), *Vv*TnPIP2;2 (HQ913642), *Vv*PnPIP2;3 (CAO18152), *Vv*TnPIP2;3 (KJ697716), *Vv*PnTIP1;1 (CAO69259), *Vv*TnTIP1;1 (KJ697717), *Vv*PnTIP2;1 (CAO45860), *Vv*TnTIP2;1 (HQ913640), *Vv*PnTIP2;2 (CAO23095), *Vv*TnTIP2;2 (KJ697718), *Vv*PnTIP4;1 (CAO44039), *Vv*TnTIP4;1 (KJ697719), *Zm*PIP2;1 (Q84RL7), *Zm*PIP2;4 (Q9ATM6), *Zm*PIP2;5 (Q9XF58). *At*: *Arabidopsis*

thaliana, *Fa*: *Fragaria*×*ananassa*, *Pv*: *Phaseolus vulgaris*, *So*: *Spinacia oleracea*, *Vv*Pn: *Vitis vinifera* cv. Pinot noir, *Vv*Tn: *V. vinifera* cv. Touriga nacional, *Zm*: *Zea mays*.
(PDF)

Figure S5 Mercury sensitive site and pH regulation site in TIPs. Alignment of TIPs aquaporins for (A) mercury sensitive site (Cys residue) and (B) pH regulation site (His residue) for gating. Consensus sequences are framed and conserved residues are indicated as red triangle. TIPs cloned in the present study are marked with red arrows. Accession numbers of presented protein sequences are: *At*-deltaTIP2 CAB10515), *At*-gammaTIP3 (AAC62778), *At*-alphaTIP (AAC42249), *Pv*-alphaTIP (CAA44669), *Vv*PnTIP1;1 (CAO69259), *Vv*TnTIP1;1 (KJ697717), *Vv*PnTIP2;1 (CAO45860), *Vv*TnTIP2;1 (HQ913640), *Vv*PnTIP2;2 (CAO23095), *Vv*TnTIP2;2 (KJ697718), *Vv*PnTIP4;1 (CAO44039), *Vv*TnTIP4;1 (KJ697719). *At*: *Arabidopsis thaliana*, *Pv*: *Phaseolus vulgaris*, *Vv*Pn: *Vitis vinifera* cv. Pinot noir, *Vv*Tn: *V. Vinifera* (cv. Touriga nacional).
(PDF)

Figure S6 Consensus sequences for transport of boron and CO_2. Alignment of putative amino acids of aquaporins of *V. Vinifera* (cv. Touriga nacional) obtained from present study and previous study [17] with the sequences of aquaporins reported to transport (A) boron and (B) CO_2. ar/R constrictions and P1–P5 positions are shown to demonstrate the conserved amino acid residue. Accession numbers of presented protein sequences are: *At*PIP1;2 (Q06611), *At*NIP5;1 (NP_192776), *Hv*PIP1;3 (BAA23745), *Hv*PIP2;1 (BAA23744), *Nt*AQP1 (O24662), *Os*-NIP2;1 (Q6Z2T3), *Vv*TnPIP1;1 (HQ913643), *Vv*TnPIP1;4 (KJ697714), *Vv*TnPIP2;1 (KJ697715), *Vv*TnPIP2;2 (HQ913642), *Vv*TnPIP2;3 (KJ697716), *Vv*TnTIP1;1 (KJ697717), *Vv*TnTIP2;1 (HQ913640), *Vv*TnTIP2;2 (KJ697718), *Vv*TnTIP4;1 (KJ697719), *Zm*PIP1;1 (Q41870). *At*: *Arabidopsis thaliana*, *Hv*: *Hordeum vulgare*, *Vv*Tn: *V. vinifera* (cv. Touriga nacional), *Zm*: *Zea mays*.
(PDF)

Figure S7 Consensus sequences for transport of ammonia. Alignment of putative amino acids of aquaporins of *V. Vinifera* (cv. Touriga nacional) obtained from present study and previous study [17] with sequences of aquaporins reported to transport ammonia. ar/R constrictions and P1–P5 positions are shown to demonstrate the conserved amino acid residue. Accession numbers of presented protein sequences are: *At*TIP2;1 (Q41951), *At*TIP2;3 (Q9FGL2), *Gm*NOD26 (P08995), *Ta*TIP2;1 (AAS19468),*Vv*TnPIP1;1 (HQ913643), *Vv*TnPIP1;4 (KJ697714), *Vv*TnPIP2;1 (KJ697715), *Vv*TnPIP2;2 (HQ913642), *Vv*TnPIP2;3 (KJ697716), *Vv*TnTIP1;1 (KJ697717), *Vv*TnTIP2;1 (HQ913640), *Vv*TnTIP2;2 (KJ697718), *Vv*TnTIP4;1 (KJ697719). *At*: *Arabidopsis thaliana*, *Gm*: *Glycine max*, *Ta*: *Triticum aestivum*, *Vv*Tn: *V. Vinifera* (cv. Touriga nacional).
(PDF)

Figure S8 Consensus sequences for transport of H_2O_2 and urea. Alignment of putative amino acids of aquaporins of *V. Vinifera* (cv. Touriga nacional) obtained from present study and previous study [17] with sequences of aquaporins reported to transport (A) H_2O_2 and (B) urea. ar/R constrictions and P1–P5 positions are shown to demonstrate the conserved amino acid residue. Accession numbers of presented protein sequences are: *At*TIP1;1 (P25818), *At*TIP1;2 (Q41963), *At*TIP1;3 (NP_192056), *At*TIP2;1 (Q41951), *At*TIP2;3 (Q9FGL2), *At*PIP2;4 (Q9FF53), *Cp*NIP1 (CAD67694), *Nt*AQP1 (O24662), *Nt*TIPa (Q9XG70), *Os*NIP2;1 (Q6Z2T3), *Vv*TnPIP1;1 (HQ913643), *Vv*TnPIP1;4 (KJ697714), *Vv*TnPIP2;1 (KJ697715), *Vv*TnPIP2;2 (HQ913642), *Vv*TnPIP2;3 (KJ697716), *Vv*TnTIP1;1 (KJ697717), *Vv*TnTIP2;1 (HQ913640), *Vv*TnTIP2;2 (KJ697718), *Vv*TnTIP4;1 (KJ697719), *Zm*PIP1;5 (Q9AR14). *At*: *Arabidopsis thaliana*, *Cp*: *Cucurbita pepo*, *Nt*: *Nicotiana tabacum*, *Os*: *Oryza sativa*, *Vv*Tn: *Vitis vinifera* (cv. Touriga nacional), *Zm*: *Zea mays*.
(PDF)

Table S1 Primers used in this work (restriction sites are underlined).
(PDF)

Acknowledgments

We thank Sara Amâncio and Luísa Carvalho, ISA-ULisboa for providing cDNAs of *V. vinifera* cv. Touriga nacional.

Author Contributions

Conceived and designed the experiments: FS MJL MCD TFM GS CP. Performed the experiments: FS MJL APM CP. Analyzed the data: FS APM MCD TFM GS CP. Contributed reagents/materials/analysis tools: MCD GS. Contributed to the writing of the manuscript: FS MJL APM MCD TFM GS CP.

References

1. Vandeleur RK, Mayo G, Shelden MC, Gilliham M, Kaiser BN, et al. (2009) The role of plasma membrane intrinsic protein aquaporins in water transport through roots: diurnal and drought stress responses reveal different strategies between isohydric and anisohydric cultivars of grapevine. Plant Physiol 149: 445–460.
2. Danielson JA, Johanson U (2008) Unexpected complexity of the aquaporin gene family in the moss *Physcomitrella patens*. BMC Plant Biol 8: 45.
3. Maurel C, Verdoucq L, Luu DT, Santoni V (2008) Plant aquaporins: membrane channels with multiple integrated functions. Annu Rev Plant Biol 59: 595–624.
4. Hove RM, Bhave M (2011) Plant aquaporins with non-aqua functions: deciphering the signature sequences. Plant Mol Biol 75: 413–430.
5. Maurel C, Chrispeels MJ (2001) Aquaporins. A molecular entry into plant water relations. Plant Physiol 125: 135–138.
6. Chaumont F, Moshelion M, Daniels MJ (2005) Regulation of plant aquaporin activity. Biol Cell 97: 749–764.
7. Soveral G, Madeira A, Loureiro-Dias MC, Moura TF (2008) Membrane tension regulates water transport in yeast. Biochim Biophys Acta 1778: 2573–2579.
8. Baiges I, Schäffner A, Mas A (2001) Eight cDNA encoding putative aquaporins in *Vitis* hybrid Richter-110 and their differential expression. J Exp Bot 52: 1949–1951.
9. Flexas J, Galmés J, Gallé A, Gulías J, Pou A, et al. (2010) Improving water use efficiency in grapevines: potential physiological targets for biotechnological improvement. Aust J Grape and Wine 16: 106–121.
10. Hayes MA, Davies C, Dry IB (2007) Isolation, functional characterization, and expression analysis of grapevine (*Vitis vinifera* L.) hexose transporters: differential roles in sink and source tissues. J Exp Bot 58: 1985–1997.
11. Jaillon O, Aury JM, Noel B, Policriti A, Clepet C, et al. (2007) The grapevine genome sequence suggests ancestral hexaploidization in major angiosperm phyla. Nature 449: 463–467.
12. Shelden MC, Howitt SM, Kaiser BN, Tyerman SD (2009) Identification and functional characterisation of aquaporins in the grapevine, *Vitis vinifera*. Funct Plant Biol 36: 1065–1078.
13. Gambetta G, Manuck C, Drucker S, Shaghasi T, Fort K, et al. (2012) The relationship between root hydraulics and scion vigour across *Vitis* rootstocks: what role do root aquaporins play? J Exp Bot 63: 6445–6455.
14. Galmés J, Pou A, Alsina MM, Tomàs M, Medrano H, et al. (2007) Aquaporin expression in response to different water stress intensities and recovery in Richter-110 (*Vitis* sp.): relationship with ecophysiological status. Planta 226: 671–681.
15. Pou A, Medrano H, Flexas J, Tyerman SD (2013) A putative role for TIP and PIP aquaporins in dynamics of leaf hydraulic and stomatal conductances in grapevine under water stress and re-watering. Plant Cell Environ 36: 828–843.
16. Fouquet R, Leon C, Ollat N, Barrieu F (2008) Identification of grapevine aquaporins and expression analysis in developing berries. Plant Cell Rep 27: 1541–1550.

17. Leitão L, Prista C, Moura TF, Loureiro-Dias MC, Soveral G (2012) Grapevine aquaporins: gating of a tonoplast intrinsic protein (TIP2;1) by cytosolic pH. PLoS One 7: e33219.
18. Noronha H, Agasse A, Martins AP, Berny MC, Gomes D, et al. (2014) The grape aquaporin VvSIP1 transports water across the ER membrane. J Exp Bot 65: 981–993.
19. Pettersson N, Hagstrom J, Bill RM, Hohmann S (2006) Expression of heterologous aquaporins for functional analysis in *Saccharomyces cerevisiae*. Curr Genet 50: 247–255.
20. Soveral G, Madeira A, Loureiro-Dias MC, Moura TF (2007) Water transport in intact yeast cells as assessed by fluorescence self-quenching. Appl Environ Microbiol 73: 2341–2343.
21. Güldener U, Hegemann J (1998) A second generation of GFP-vectors for subcellular localization studies in budding yeast. Technical report, Heinrich-Heine Universität, Inst. für Mikrobiologie. Available: http://mips.helmholtz-muenchen.de/proj/yeast/info/tools/hegemann/gfp.html Accessed 2014 April 16.
22. Hanahan D (1985) Techniques for transformation of *E. coli*. In DNA cloning: A Practical Approach. (ed DM Glover) 1: 109–135.
23. Pronk JT (2002) Auxotrophic yeast strains in fundamental and applied research. Appl Environ Microbiol 68: 2095–2100.
24. Thompson JD, Gibson TJ, Plewniak F, Jeanmougin F, Higgins DG (1997) The CLUSTAL_X windows interface: flexible strategies for multiple sequence alignment aided by quality analysis tools. Nucleic Acids Res 25: 4876–4882.
25. Hall TA (1999) BioEdit: a user-friendly biological sequence alignment editor and analysis program for Windows 95/98/NT 41: 95–98.
26. Tamura K, Peterson D, Peterson N, Stecher G, Nei M, et al. (2011) MEGA5: molecular evolutionary genetics analysis using maximum likelihood, evolutionary distance, and maximum parsimony methods. Mol Biol Evol 28: 2731–2739.
27. Krogh A, Larsson B, von Heijne G, Sonnhammer EL (2001) Predicting transmembrane protein topology with a hidden Markov model: application to complete genomes. J Mol Biol 305: 567–580.
28. Tusnady GE, Simon I (2001) The HMMTOP transmembrane topology prediction server. Bioinformatics 17: 849–850.
29. Hofmann K, Stoffel W (1993) TMbase - A database of membrane spanning proteins segments. Biol Chem Hoppe-Seyler 374: 166.
30. Johanson U, Karlsson M, Johansson I, Gustavsson S, Sjövall S, et al. (2001) The complete set of genes encoding major intrinsic proteins in *Arabidopsis* provides a framework for a new nomenclature for major intrinsic proteins in plants. Plant Physiol 126: 1358–1369.
31. Forrest KL, Bhave M (2007) Major intrinsic proteins (MIPs) in plants: a complex gene family with major impacts on plant phenotype. Funct Integr Genomics 7: 263–289.
32. Froger A, Tallur B, Thomas D, Delamarche C (1998) Prediction of functional residues in water channels and related proteins. Protein Sci 7: 1458–1468.
33. Heymann JB, Engel A (2000) Structural clues in the sequences of the aquaporins. J Mol Biol 295: 1039–1053.
34. Johansson I, Karlsson M, Johanson U, Larsson C, Kjellbom P (2000) The role of aquaporins in cellular and whole plant water balance. Biochim Biophys Acta 1465: 324–342.
35. Santoni V, Verdoucq L, Sommerer N, Vinh J, Pflieger D, et al. (2006) Methylation of aquaporins in plant plasma membrane. Biochem J 400: 189–197.
36. Zelazny E, Miecielica U, Borst JW, Hemminga MA, Chaumont F (2009) An N-terminal diacidic motif is required for the trafficking of maize aquaporins ZmPIP2;4 and ZmPIP2;5 to the plasma membrane. Plant J 57: 346–355.
37. Tournaire-Roux C, Sutka M, Javot H, Gout E, Gerbeau P, et al. (2003) Cytosolic pH regulates root water transport during anoxic stress through gating of aquaporins. Nature 425: 393–397.
38. Nyblom M, Frick A, Wang Y, Ekvall M, Hallgren K, et al. (2009) Structural and functional analysis of SoPIP2;1 mutants adds insight into plant aquaporin gating. J Mol Biol 387: 653–668.
39. Van Wilder V, Miecielica U, Degand H, Derua R, Waelkens E, et al. (2008) Maize plasma membrane aquaporins belonging to the PIP1 and PIP2 subgroups are *in vivo* phosphorylated. Plant Cell Physiol 49: 1364–1377.
40. Prak S, Hem S, Boudet J, Viennois G, Sommerer N, et al. (2008) Multiple phosphorylations in the C-terminal tail of plant plasma membrane aquaporins role in subcellular trafficking of AtPIP2; 1 in response to salt stress. Mol Cell Proteomics 7: 1019–1030.
41. Johansson I, Karlsson M, Shukla VK, Chrispeels MJ, Larsson C, et al. (1998) Water transport activity of the plasma membrane aquaporin PM28A is regulated by phosphorylation. The Plant Cell Online 10: 451–459.
42. Daniels MJ (1996) Characterization of a new vacuolar membrane aquaporin sensitive to mercury at a unique site. Plant Cell 8: 587–599.
43. Kjellbom P, Larsson C, Johansson I, Karlsson M, Johanson U (1999) Aquaporins and water homeostasis in plants. Trends Plant Sci 4: 308–314.
44. Wudick MM, Luu DT, Maurel C (2009) A look inside: localization patterns and functions of intracellular plant aquaporins. New Phytol 184: 289–302.
45. Maurel C, Reizer J, Schroeder J, Chrispeels M (1993) The vacuolar membrane protein gamma-TIP creates water specific channels in *Xenopus* oocytes. The EMBO Journal 12: 2241–2247.
46. Daniels MJ, Mirkov TE, Chrispeels MJ (1994) The plasma membrane of *Arabidopsis thaliana* contains a mercury-insensitive aquaporin that is a homolog of the tonoplast water channel protein TIP. Plant Physiol 106: 1325–1333.
47. Suga S, Maeshima M (2004) Water channel activity of radish plasma membrane aquaporins heterologously expressed in yeast and their modification by site-directed mutagenesis. Plant Cell Physiol 45: 823–830.
48. Neill S, Desikan R, Hancock J (2002) Hydrogen peroxide signalling. Curr Opin Plant Biol 5: 388–395.
49. Antunes F, Cadenas E, Brunk U (2001) Apoptosis induced by exposure to a low steady-state concentration of H_2O_2 is a consequence of lysosomal rupture. Biochem J 356: 549–555.
50. Bienert GP, Schjoerring JK, Jahn TP (2006) Membrane transport of hydrogen peroxide. Biochim Biophys Acta - Biomembranes 1758: 994–1003.
51. Bienert GP, Møller ALB, Kristiansen KA, Schulz A, Møller IM, et al. (2007) Specific aquaporins facilitate the diffusion of hydrogen peroxide across membranes. J Biol Chem 282: 1183–1192.
52. Dynowski M, Schaaf G, Loque D, Moran O, Ludewig U (2008) Plant plasma membrane water channels conduct the signalling molecule H_2O_2. Biochem J 414: 53–61.
53. Bienert GP, Heinen RB, Berny MC, Chaumont F (2014) Maize plasma membrane aquaporin ZmPIP2;5, but not ZmPIP1;2, facilitates transmembrane diffusion of hydrogen peroxide. Biochim Biophys Acta 1838: 216–222.
54. Mori IC, Schroeder JI (2004) Reactive oxygen species activation of plant Ca^{2+} channels. A signaling mechanism in polar growth, hormone transduction, stress signaling, and hypothetically mechanotransduction. Plant Physiol 135: 702–708.
55. Foyer CH, Noctor G (2003) Redox sensing and signalling associated with reactive oxygen in chloroplasts, peroxisomes and mitochondria. Physiol Plant 119: 355–364.
56. Boursiac Y, Boudet J, Postaire O, Luu DT, Tournaire-Roux C, et al. (2008) Stimulus-induced downregulation of root water transport involves reactive oxygen species-activated cell signalling and plasma membrane intrinsic protein internalization. Plant J 56: 207–218.
57. Azad AK, Yoshikawa N, Ishikawa T, Sawa Y, Shibata H (2012) Substitution of a single amino acid residue in the aromatic/arginine selectivity filter alters the transport profiles of tonoplast aquaporin homologs. Biochim Biophys Acta 1818: 1–11.
58. Azad A, Ishikawa T, Ishikawa T, Sawa Y, Shibata H (2008) Intracellular energy depletion triggers programmed cell death during petal senescence in tulip. J Exp Bot 59: 2085–2095.
59. Canetta E, Walker GM, Adya AK (2009) Nanoscopic morphological changes in yeast cell surfaces caused by oxidative stress: an atomic force microscopic study. J Microbiol Biotechnol 19: 547–555.
60. Kuthan M, Devaux F, Janderová B, Slaninová I, Jacq C, et al. (2003) Domestication of wild *Saccharomyces cerevisiae* is accompanied by changes in gene expression and colony morphology. Mol Microbiol 47: 745–754.
61. Dordas C, Chrispeels MJ, Brown PH (2000) Permeability and channel-mediated transport of boric acid across membrane vesicles isolated from squash roots. Plant Physiol 124: 1349–1362.
62. Fitzpatrick KL, Reid RJ (2009) The involvement of aquaglyceroporins in transport of boron in barley roots. Plant Cell Environ 32: 1357–1365.
63. Takano J, Wada M, Ludewig U, Schaaf G, von Wiren N, et al. (2006) The *Arabidopsis* major intrinsic protein NIP5;1 is essential for efficient boron uptake and plant development under boron limitation. Plant Cell 18: 1498–1509.
64. Tanaka M, Wallace IS, Takano J, Roberts DM, Fujiwara T (2008) NIP6;1 is a boric acid channel for preferential transport of boron to growing shoot tissues in *Arabidopsis*. Plant Cell 20: 2860–2875.
65. Mitani N, Yamaji N, Ma JF (2008) Characterization of substrate specificity of a rice silicon transporter, Lsi1. Pflugers Arch, EJP 456: 679–686.
66. Schnurbusch T, Hayes J, Hrmova M, Baumann U, Ramesh SA, et al. (2010) Boron toxicity tolerance in barley through reduced expression of the multifunctional aquaporin HvNIP2;1. Plant Physiol 153: 1706–1715.
67. Tanaka M, Fujiwara T (2008) Physiological roles and transport mechanisms of boron: perspectives from plants. Pflugers Arch 456: 671–677.
68. Nozawa A, Takano J, Kobayashi M, von Wiren N, Fujiwara T (2006) Roles of *BOR1*, *DUR3*, and *FPS1* in boron transport and tolerance in *Saccharomyces cerevisiae*. FEMS Microbiol Lett 262: 216–222.